

Parametric Instability Driven by Weakly Trapped Particles in Nonlinear Plasma Waves

Daniel H. E. Dubin

Department of Physics, UCSD, La Jolla, California 92093, USA

 (Received 11 April 2018; published 3 July 2018)

This Letter describes a new parametric instability mechanism caused by a distribution f_T of particles trapped in the potential wells of a wave train. The mechanism explains a nonlinear instability in Trivelpiece-Gould (TG) waves, and it could also be a destabilizing factor in a range of nearly collisionless nonlinear plasma waves. The theory is compared to particle in cell simulations of TG waves.

DOI: 10.1103/PhysRevLett.121.015001

Many plasmas exhibit parametric instabilities, in which longer-wavelength “daughter waves” grow on a shorter-wavelength nonlinear “pump” wave. The instability has been observed in laser-plasma experiments [1,2] in tokamaks [3,4] and other magnetic confinement devices [5,6], and in non-neutral plasmas [7–9], and it has been studied in theory and simulation for many years in a range of scenarios [10–15]. Here, we consider a novel instability mechanism caused by particles trapped in, and carried along by, the fields of the pump wave. The instability mechanism is quite simple and fairly general and may therefore be applicable to a range of nonlinear wave phenomena in which particles are trapped in the wave.

The mechanism applies to waves with a nearly acoustic dispersion relation, $\omega(k) \approx ck$, in which the pump wave decays to daughter waves of the same type (i.e., on the same branch of the dispersion relation). This case describes experiments [7,8] involving large-amplitude Trivelpiece-Gould (TG) plasma waves [16,17] traveling axially along a non-neutral plasma column. Under these circumstances, it has been previously shown that the classic three-wave theory of parametric instability [10], based on ideal fluid equations, is inapplicable; and that, in fact, ideal fluid theory predicts that the pump wave is stable at all amplitudes [18]. We show that parametric instability arises when “weakly trapped” particles are included in the theory. We compare these results to particle in cell (PIC) simulations, which observe parametric instability only when such weakly trapped particles are present, at a growth rate consistent with the new theory.

The instability mechanism is as follows. Consider a nonlinear pump wave with amplitude A , wave number k , and phase speed u [19]. The growth of daughter waves with wave number $k/2$ and speed close to u (the most unstable case) corresponds to a slow relative motion of the pump wave peaks; pairs of adjacent peaks approach one another and recede from neighboring pairs. Any particles trapped between the approaching peaks of the pump wave are adiabatically heated, while any particles trapped between receding peaks are cooled.

This heating and cooling would normally produce restoring forces that stabilize the relative motion of the peaks. However, some weakly trapped particles are heated enough to become untrapped, and these particles are then retrapped and cooled between receding peaks (an untrapped particle moving toward a receding peak can reflect from it and lose energy, becoming trapped). The net effect of this detraping and retrapping is to change the sign of the restoring force, producing a trapped-particle force that *amplifies* the modulations.

A simplified model for this process applies to pump waves made up of a chain of solitonlike potential peaks, each separated by a large wavelength L compared to their width. Each potential well in the chain has a trapped-particle distribution $f_T(v)$ [Fig. 1(a)]. Consider the trapped-particle distributions $f_1(v)$ and $f_2(v)$ in adjacent wells. Initially, both f_1 and f_2 equal f_T . In the instability, the two adjacent peaks that trap f_1 slowly reduce their separation

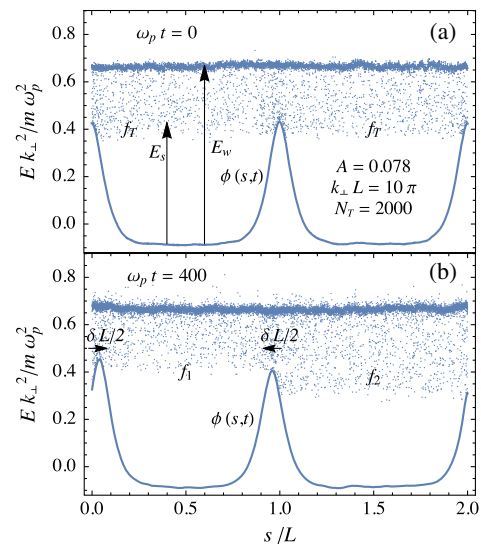


FIG. 1. PIC simulation showing energy versus position in a TG wave with trapped particles, at two times. (a) $\omega_p t = 0$; (b) $\omega_p t = 400$.

by δL . The next peaks recede from one another by the same distance δL [Fig. 1(b)]. This motion is replicated along the wave train, creating a periodic structure with period $2L$ (the daughter waves, with twice the pump wavelength).

Trapped particles are adiabatically compressed in the first well, and $f_1(v)$ changes from $f_T(v)$ to $f_T(vL_1/L) \equiv f_1^{\text{final}}(v)$, where $L_1 = L - \delta L$. The density change for these particles is $\delta n_1 = 2 \int_0^{v_s} dv (f_1^{\text{final}} - f_T)$, where v_s is the separatrix speed, given in terms of the peak height E_s by $mv_s^2/2 = E_s$. Taylor expansion to first order in δL and integration by parts gives the density change as

$$\delta n_1 = 2 \frac{\delta L}{L} \int_0^{v_s} dv [f_T(v) - f_T(v_s)]. \quad (1)$$

If $f_T(v_s) = 0$, the density change in the compression is positive. However, for weakly trapped particles with a distribution satisfying $f_T(v_s) \geq f_T(v)$ for $|v| < v_s$, δn_1 is *negative* under compression. This occurs because particles escape the potential well as they are heated [Fig. 1(b)].

The trapped-particle distribution $f_2(v)$ between the receding peaks can be analyzed the same way. This distribution changes from $f_T(v)$ to

$$f_2^{\text{final}}(v) = \begin{cases} f_T(vL_2/L), & 0 < v < v_s L/L_2 \\ f_T(2v_s - vL_2/L), & v_s L/L_2 < v < v_s \end{cases}, \quad (2)$$

where $L_2 = L + \delta L$. The second form for f_2 is from particles retrapped from the other well.

The total kinetic energy change $\delta E_T = \delta E_1 + \delta E_2$ for these trapped particles is

$$\delta E_T = 2 \int_0^{v_s} dv \frac{mv^2}{2} [L_1 f_1^{\text{final}} + L_2 f_2^{\text{final}} - 2L f_T(v)], \quad (3)$$

After Taylor expansion and integration by parts, one finds that δE_T is second order in δL (as expected since $\pm \delta L$ must give the same energy change): $\delta E_T = -\beta \delta L^2$, where

$$\beta = \frac{6}{L} \int_0^{v_s} dv m v^2 [f_T(v_s) - f_T(v)]. \quad (4)$$

For a weakly trapped distribution with $\beta > 0$, the process reduces the kinetic energy of the trapped particles. This energy change can drive the instability.

An approximate expression for the decay instability growth rate can now be found by treating the wave train as a chain of solitons. A soliton's energy E_0 is a function of its speed u . Adjacent solitons change velocities by $+\delta u$ and $-\delta u$, respectively, where $\delta u = (1/2)d\delta L/dt$. Then the energy change per pair is $\delta E_0 = \alpha(\delta u)^2$, where $\alpha = \partial^2 E_0 / \partial u^2 > 0$ is the ‘‘inertial mass’’ of a soliton. This energy change is due to the work done by trapped particles, and energy conservation $\delta E_0 + \delta E_T = 0$ implies the ordinary differential equation (ODE)

$$\alpha(\delta \dot{L}/2)^2 - \beta(\delta L)^2 = 0. \quad (5)$$

This ODE yields an exponential growth rate Γ for $\delta L(t)$ given by $\Gamma = 2\sqrt{\beta/\alpha}$. (There is also an exponentially decaying solution with decay rate Γ .) The growth rate in this model is proportional to the square root of the number of trapped particles, and instability occurs for any number of trapped particles, no matter how small (provided that $\beta > 0$, i.e., that the distribution is weakly trapped).

This simple model can be made somewhat more realistic by noting that, in the ideal fluid model of nonlinear TG waves, interacting solitons repel (the solitons are elevated density regions of like-sign charge) [18]. The repulsion adds a restoring energy $\kappa(\delta L)^2$ per pair to the energy of the chain of solitons, and hence to Eq. (5):

$$\alpha(\delta \dot{L}/2)^2 + \kappa(\delta L)^2 - \beta(\delta L)^2 = 0, \quad (6)$$

which implies the growth rate is modified to

$$\Gamma = 2\sqrt{(\beta - \kappa)/\alpha}. \quad (7)$$

Now instability requires that the trapped-particle fraction must be sufficiently large to overcome the natural repulsion between wave density peaks.

A more general kinetic theory of the instability applies to waves of any amplitude or wavelength, and treats the system as a cold fluid plus a weak tail distribution that includes trapped particles. Neglecting tail particles, the nonlinear wave is assumed to be a steady solution of the cold fluid equations [18] with density $n(s)$, fluid velocity $V(s)$, and potential $\phi(s) = \hat{G}n$, as seen in the wave frame, where \hat{G} is the Green's function operator for Poisson's equation. The tail particles are treated as a perturbation. The tail distribution function f_T is assumed to evolve adiabatically in the wave potential. The initial tail distribution is a function of particle energy, $f_T = f_T(E)$, where $E = mv^2/2 + \phi(s)$, and v is particle velocity in the wave frame. Collisionless adiabatic theory implies that changes in the tail distribution, caused by changes $\delta\phi(s, t)$ in the wave potential, are

$$\delta f_T(s, v, t) = \frac{\partial f_T}{\partial E} [\delta\phi(s, t) - \langle \delta\phi \rangle(E, t)], \quad (8)$$

where $\langle \cdot \rangle$ is an average along a particle trajectory in phase space holding energy E fixed [20].

The cold fluid evolves according to fluid equations coupled to the tail particles via the wave potential. The perturbed fluid velocity $\delta V(s, t)$ and density $\delta n(s, t)$ follow linearized continuity and momentum equations,

$$\frac{\partial}{\partial t} \begin{pmatrix} \delta n \\ \delta V \end{pmatrix} + \frac{\partial}{\partial s} \begin{pmatrix} V\delta n + n\delta V \\ V\delta V + \delta\phi_F/m \end{pmatrix} = -\frac{\partial}{\partial s} \begin{pmatrix} 0 \\ \delta\phi_T/m \end{pmatrix}. \quad (9)$$

Here, we have broken the perturbed wave potential $\delta\phi$ into two pieces, a fluid portion $\delta\phi_F \equiv \hat{G}\delta n$ and a portion $\delta\phi_T \equiv \hat{G}\delta n_T$ arising from the tail density $\delta n_T = \int dv \delta f_T$, using Eq. (8) for δf_T .

To analyze the stability of solutions to Eq. (9), consider the eigenmodes of the equation. Let $\psi_0(s) \equiv (\delta n_0(s), \delta V_0(s))$ be a complex vector eigenfunction of Eq. (9) with no tail particles ($\delta\phi_T = 0$). That is, ψ_0 satisfies

$$i\omega_0\psi_0 = \hat{L} \cdot \psi_0, \quad (10)$$

with a linear matrix operator $\hat{L} \equiv (\partial/\partial s) \begin{pmatrix} V & n \\ \hat{G}/m & V \end{pmatrix}$, where ω_0 is the eigenfrequency.

The operator \hat{L} is anti-Hermitian with respect to a matrix inner product: for any two eigenfunctions ψ_1 and ψ_2 , $[\psi_1, \hat{L} \cdot \psi_2] = -[\psi_2, \hat{L} \cdot \psi_1]^*$, where

$$[\psi_1, \psi_2] = \int ds \psi_1^* \cdot \begin{pmatrix} \hat{G}^\dagger & mV \\ mV & mn \end{pmatrix} \cdot \psi_2, \quad (11)$$

and where \hat{G}^\dagger is the left Green's function operator defined as $\delta\phi = \delta n \hat{G}^\dagger$. The anti-Hermitian property of \hat{L} implies that [21] (i) all eigenfrequencies are real; (ii) ψ_0^* is also an eigenfunction with eigenfrequency $-\omega_0$; and (iii) $[\psi_0, \psi_0^*] = 0$, provided $\omega_0 \neq 0$. Result (i) implies that steady traveling wave solutions to the cold fluid equations are stable, from which it follows that three-wave theory for parametric instability [10] cannot apply to this system, conclusions found via a more circuitous route in Dubin and Ashourvan [18,22].

Furthermore, Eq. (11) implies that $[\psi_0, \psi_0]$ is real and is equal to 4 times the eigenmode energy δE_0 :

$$\begin{aligned} [\psi_0, \psi_0] &= 4\delta E_0 \\ &= \int ds \{ nm |\delta V_0|^2 + mV (\delta n_0 \delta V_0^* + \delta V_0 \delta n_0^*) \\ &\quad + \delta n_0 \delta \phi_0^* \}, \end{aligned} \quad (12)$$

where $\delta\phi_0 \equiv \hat{G}\delta n_0$ is the eigenmode potential. (The reality of δE_0 follows from the symmetry $\int ds \delta n_1 \hat{G} \delta n_2 = \int ds \delta n_2 \hat{G} \delta n_1$ for any δn_1 and δn_2 .)

The effect of the tail particles can now be handled with degenerate perturbation theory, assuming that the fraction of tail particles is small. Including these particles, an eigenmode $\psi \equiv (\delta n, \delta V)$ of Eq. (9), with frequency ω , satisfies

$$i\omega\psi = \hat{L} \cdot \psi + \hat{C} \cdot \psi, \quad (13)$$

where $\hat{C} \cdot \psi \equiv (\partial/\partial s)(0, \delta\phi_T/m)$ is treated as a small perturbation. Then the most unstable eigenmode will be perturbed away from the unperturbed pair (ψ_0, ψ_0^*) that has the smallest frequencies $(\omega_0, -\omega_0)$. In degenerate perturbation theory, we write $\psi = a\psi_0 + b\psi_0^* + \Delta\psi$,

where $[\psi_0, \Delta\psi] = [\psi_0^*, \Delta\psi] = 0$, and where $\Delta\psi$ is small. Substituting for ψ in Eq. (13), using Eq. (10) and its complex conjugate, and dropping the small term $\hat{C} \cdot \Delta\psi$ yields

$$\begin{aligned} i\omega(a\psi_0 + b\psi_0^* + \Delta\psi) \\ = i\omega_0(a\psi_0 - b\psi_0^*) + \hat{L} \cdot \Delta\psi + a\hat{C} \cdot \psi_0 + b\hat{C} \cdot \psi_0^*. \end{aligned} \quad (14)$$

Taking inner products of this equation with respect to ψ_0 and ψ_0^* , the $\Delta\psi$ terms vanish and one obtains two coupled homogeneous equations for the coefficients a and b , which can be written in matrix form as $\mathbf{M} \cdot (a, b) = (0, 0)$. Setting the determinant of the matrix \mathbf{M} to zero determines the eigenfrequency ω as $\omega^2 = \omega_0^2 - (X + X^*)\omega_0 + |Y|^2 - |X|^2$, where $X = i[\psi_0, \hat{C} \cdot \psi_0]/[\psi_0, \psi_0]$ and $Y = i[\psi_0, \hat{C} \cdot \psi_0^*]/[\psi_0, \psi_0]$. Since X and Y are small, the $|Y|^2 - |X|^2$ term can be dropped, and to first order in the tail density the eigenfrequency is

$$\omega^2 = \omega_0^2 - 2X\omega_0, \quad (15)$$

where we take X to be real (this is shown later). Instability occurs when $X > \omega_0/2$. The coefficient X can be directly related to the tail distribution. Using Eqs. (11) and (12),

$$\begin{aligned} X &= i \frac{\int ds (V \delta n_0^* + n \delta V_0^*) \partial \delta \phi_T / \partial s}{4\delta E_0} \\ &= -\omega_0 \frac{\int ds \delta n_0^* \delta \phi_T}{4\delta E_0} = -\omega_0 \frac{\int ds \delta \phi_0^* \delta n_T}{4\delta E_0}, \end{aligned} \quad (16)$$

where we integrated by parts and used the complex conjugate of the continuity equation [the first element of Eq. (10)], and the final form employed symmetry of the Green's function. The tail density δn_T is obtained by integrating over δf_T given by Eq. (8):

$$\delta n_T(s) = \int dv \frac{\partial f_T}{\partial E}(E) [\delta \phi_0(s) - \langle \delta \phi_0 \rangle(E)], \quad (17)$$

where for simplicity we have dropped $\delta\phi_T$ on the right-hand side, keeping only the potential $\delta\phi_0 = \hat{G}\delta n_0$ from the fluid density δn_0 in the eigenmode. We can do this because $\delta\phi_T \ll \delta\phi_0$ since the tail particle density is assumed small. Applying Eq. (17) to Eq. (16) yields

$$X = \frac{\omega_0}{4\delta E_0} \int ds dv \frac{\partial f_T}{\partial E} [|\langle \delta \phi_0 \rangle|^2 - |\delta \phi_0(s)|^2]. \quad (18)$$

Thus, the coefficient X is real and proportional to the fraction of tail particles.

We can now connect Eq. (15) to the previous expression for the growth rate, Eq. (7). In that simplified model we treated the wave train as a chain of weakly interacting solitons. As one soliton moves by $\delta L/2$ and the next moves

by $-\delta L/2$, the wave potential change in each soliton is $\delta\phi_0(s) = \pm(1/2)\delta L\partial\phi(s)/\partial s$, where $\phi(s)$ is the equilibrium soliton potential. This potential is mainly local to each soliton, and therefore the $|\delta\phi_0(s)|^2$ term in Eq. (18) is negligible compared to $|\langle\delta\phi_0\rangle|^2$. As shown in Ref. [20], the bounce average of $\delta\phi_0$ is then given by $\langle\delta\phi_0\rangle = \pm mv^2\delta L/L$ for trapped particles (those with speed $|v| < v_s$), and it is zero for untrapped particles, where the upper (lower) sign is for compressing (expanding) potential wells. Applying this to Eq. (18) and integrating in v and in s over one pair of wells (of length $2L$) yields $2\omega_0 X = (\omega_0\delta L)^2\beta/\delta E_0$, where β is given by Eq. (4). Here, we have used $E = mv^2/2$, $\partial f_T/\partial E = (1/mv)\partial f_T/\partial v$, and we have performed an integration by parts in v . Substituting for $2\omega_0 X$ in Eq. (15) and again taking $\delta E_0 = \alpha(\delta u)^2$, where $|\delta u| = \omega_0\delta L/2$ is the change in soliton speed, results in the growth rate $\Gamma = \sqrt{4\beta/\alpha - \omega_0^2}$, which is equivalent to Eq. (7).

We now compare this theory of parametric instability to PIC simulations of a nonlinear TG wave. The simulations are in the wave frame, using periodic boundary conditions with period $2L$, with $N = 10^6$ particles of charge e and mass m . The Poisson equation relating density to potential in these 1D simulations is $\partial^2\phi/\partial s^2 - k_\perp^2\phi = -4\pi e^2 n$, where k_\perp is the perpendicular wave number of the waves [8,18], a free parameter in the simulations; in Fig. 1 $k_\perp L = 10\pi$. The initial particle distribution in the wave frame (where particles are flowing to the left with mean speed u) is nearly a δ function at energy E_w above the potential minimum. The resulting density and fluid velocity create a large-amplitude wave with $A = 0.078$, stationary in this frame. To this distribution $N_T = 2000$ tail particles are added, distributed uniformly in phase space between energies from E_w down to $E_m = 0.9E_s$ [Fig. 1(a)]. This creates a population of about 400 trapped particles.

In Fig. 1(b) the distribution is shown at time $\omega_p t = 400$, where $\omega_p = \sqrt{4\pi e^2 n_0/m}$ is the plasma frequency. The wave peaks have moved spontaneously and trapped particles have been heated in the left well, causing them to become untrapped and then retrapped in the right well, where trapped particles are cooled to lower energy. The change $\delta L(t)$ in the distance between wave peaks increases exponentially with time [23], and an exponential fit gives the growth rate for the instability.

Figure 2 displays growth rates versus the number N_T of tail particles (with f_T , the same functional form as described above) for two amplitude and k_\perp values. The solid dots are growth rates measured in simulations. The lines are Eqs. (15) and (18). The fluid wave functions $n(s)$, $V(s)$, $\phi(s)$, the eigenfunction $\psi_0 = (\delta n_0, \delta V_0)$, and the frequency ω_0 are evaluated using the methods described in Ref. [18]; see Fig. 3 for examples. For the more nonlinear wave (red data) ω_0 is quite small and the simple ‘‘chain-of-solitons’’ model provides a growth rate estimate,

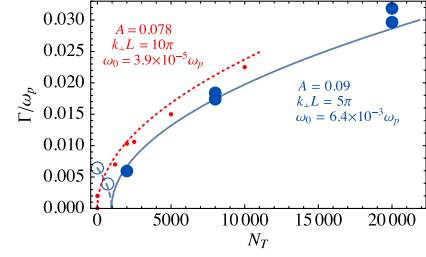


FIG. 2. Growth rates in simulations (points) and from Eq. (15) (lines) versus the number of tail particles, for two cases: red, a very nonlinear wave (ϕ shown in Fig. 1) and blue, a less nonlinear wave (see Fig. 3).

$\Gamma = 2\sqrt{\beta/\alpha}$, with β given by Eq. (4). One can show [18] that for large-amplitude TG solitons $\alpha \approx 16mn_0/k_\perp$, with $n_0 = N/(2L)$. For a uniform $f_T \approx N_T/[4L(v_w - v_m)] \equiv f_{T0}$ when $v_m < |v| < v_w$ (where $v_w = \sqrt{2E_w/m} = 1.22\omega_p/k_\perp$ and $v_m = \sqrt{2E_m/m} = 0.96\omega_p/k_\perp$), $\beta/\alpha \approx (4/16)(f_{T0}/N)k_\perp v_m^3$. This gives $\Gamma = 0.16\sqrt{N_T/N}\omega_p$, within 30% of Eq. (15). For the weaker wave (blue data) the open symbols are below the instability threshold. In these cases $\delta L(t)$ oscillated at the plotted rates, rather than exponentially increasing. The blue dashed curve is the frequency predicted by Eq. (15).

These simulations varied the number of tail particles N_T (proportional to the trapped-particle number) holding the functional form of f_T fixed, but in other simulations (not shown) the tail distribution was modified, taking $E_m > E_s$, so that there were no trapped particles. No instability was observed for any N_T , as the new theory predicts.

The parametric instability discussed in this Letter arises from a novel effect: when compressed by growing daughter waves, weakly trapped particles ‘‘change sides’’ by becoming detrapped and then retrapped and thus amplify the compression. The growth rate scales roughly as the square root of the trapped-particle fraction. Two versions of the

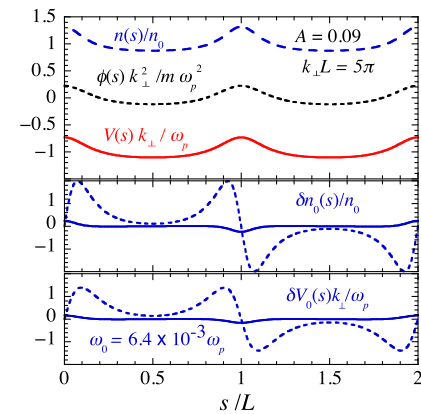


FIG. 3. (Top) Density, potential, and velocity in the cnoidal wave used for the blue data in Fig. 2. (Bottom) Least-stable fluid eigenmode. Solid lines, real; dashed lines, imaginary.

theory were presented, a chain-of-solitons model and a novel kinetic theory, and the theories were compared to PIC simulations. The simulations and theory are for traveling waves, but we have also observed similar growth rates for standing waves of relevance to previous experiments [7,8]. Future work will extend the theory to standing waves and compare to simulations and experiments. The new theory may also be relevant to other plasma waves such as Bernstein-Greene-Kruskal states [24] and electron acoustic waves [9,25], where trapped particles play a central role in the wave dynamics; ion acoustic waves, where trapped particles have been observed to affect parametric decay [14]; and waves in other systems such as 2D nearly inviscid fluids, where the exchange of vorticity across moving flow separatrices (for example, in nonlinear Kelvin waves [26–28]) may have similar consequences to the effects considered here.

The author thanks Professors T.M. O’Neil and C.F. Driscoll and Drs. F. Anderegg and M. Affolter for useful discussions. This work was supported by U.S. DOE Grants No. DE-SC0018236 and No. DE-SC0008693.

-
- [1] H. C. Bandulet, C. Labaune, K. Lewis, and S. Depierreux, *Phys. Rev. Lett.* **93**, 035002 (2004).
- [2] C. Niemann, S. H. Glenzer, J. Knight, L. Divol, E. A. Williams, G. Gregori, B. I. Cohen, C. Constantin, D. H. Froula, D. S. Montgomery, and R. P. Johnson, *Phys. Rev. Lett.* **93**, 045004 (2004).
- [3] S. G. Baek, R. R. Parker, S. Shiraiwa, G. M. Wallace, P. T. Bonoli, D. Brunner, I. C. Faust, A. E. Hubbard, B. LaBombard, and M. Porkolab, *Plasma Phys. Controlled Fusion* **55**, 052001 (2013).
- [4] M. Porkolab, S. Bernabei, W. M. Hooke, R. W. Motley, and T. Nagashima, *Phys. Rev. Lett.* **38**, 230 (1977).
- [5] R. Stenzel and A. Y. Wong, *Phys. Rev. Lett.* **28**, 274 (1972).
- [6] S. Dorfman and T. A. Carter, *Phys. Rev. Lett.* **116**, 195002 (2016).
- [7] H. Higaki, *Plasma Phys. Controlled Fusion* **39**, 1793 (1997).
- [8] M. Affolter, F. Anderegg, D. H. E. Dubin, F. Valentini, and C. F. Driscoll (to be published); F. Anderegg, M. Affolter, A. Ashourvan, D. H. E. Dubin, F. Valentini, and C. F. Driscoll, *AIP Conf. Proc.* **1668**, 020001 (2015).
- [9] A. A. Kabantsev, F. Valentini, and C. F. Driscoll, *AIP Conf. Proc.* **862**, 13 (2006).
- [10] R. Z. Sagdeev and A. A. Galeev, *Nonlinear Plasma Theory* (W.A. Benjamin, New York, 1969).
- [11] S. J. Karttunen, J. N. McMullin, and A. A. Offenberger, *Phys. Fluids* **24**, 447 (1981).
- [12] B. I. Cohen, B. F. Lasinski, A. B. Langdon, and E. A. Williams, *Phys. Plasmas* **4**, 956 (1997).
- [13] D. Pesme, C. Riconadaa, and V. T. Tikhonchuk, *Phys. Plasmas* **12**, 092101 (2005).
- [14] T. Chapman, R. L. Berger, B. I. Cohen, J. W. Banks, and S. Brunner, *Phys. Rev. Lett.* **119**, 055002 (2017).
- [15] A. Tenerani, M. Velli, and P. Hellinger, *Astrophys. J.* **851**, 99 (2017).
- [16] A. W. Trivelpiece and R. W. Gould, *J. Appl. Phys.* **30**, 1784 (1959).
- [17] R. L. Stenzel and J. M. Urrutia, *Phys. Plasmas* **23**, 092103 (2016).
- [18] D. H. E. Dubin and A. Ashourvan, *Phys. Plasmas* **22**, 102102 (2015).
- [19] Here, amplitude A is defined as the amplitude of the fundamental spatial harmonic in the scaled traveling wave density $n(s)/n_0$, where n_0 is the equilibrium density and $s = x - ut$ is position measured in the wave frame.
- [20] D. H. E. Dubin, *Phys. Plasmas* **24**, 112120 (2017).
- [21] R. Horn and C. Johnson, *Matrix Analysis* (Cambridge University Press, Cambridge, England, 1985).
- [22] Incidentally, this method can be adapted to examine the stability of cnoidal waves in other nonlinear wave systems, such as the Korteweg–de Vries and Boussinesq equations. It is a less comprehensive but arguably more straightforward approach than methods based on inverse scattering [C. S. Gardner, J. M. Greene, M. D. Kruskal, and R. M. Miura, *Commun. Pure Appl. Math.* **27**, 97 (1974)] that are typically used to analyze general solutions to such equations.
- [23] See Supplemental Material at <http://link.aps.org/supplemental/10.1103/PhysRevLett.121.015001> for an animation of the potential and particle energy in a PIC simulation showing the linear and nonlinear phases of the instability of the plasma in Fig. 1.
- [24] I. B. Bernstein, J. M. Green, and M. D. Kruskal, *Phys. Rev.* **108**, 546 (1957).
- [25] F. Valentini, T. M. O’Neil, and D. H. E. Dubin, *Phys. Plasmas* **13**, 052303 (2006).
- [26] T. B. Mitchell and C. F. Driscoll, *Phys. Rev. Lett.* **73**, 2196 (1994).
- [27] D. A. Schecter, D. H. E. Dubin, A. C. Cass, C. F. Driscoll, I. M. Lansky, and T. M. O’Neil, *Phys. Fluids* **12**, 2397 (2000).
- [28] N. C. Hurst, J. R. Danielson, D. H. E. Dubin, and C. M. Surko, *Phys. Rev. Lett.* **117**, 235001 (2016).